Nonlinear spectral-phase-engineering strategies via quasiparametric chirped-pulse amplification

Ji Wang [1,2] Yunlin Chen [1,*] Kun Zhao,[2] and Zhiyi Wei[2]
[1]Institute of Applied Mic-Nano Materials, School of Science, Beijing Jiaotong University, Beijing 100044, China
[2]Institute of Physics, Chinese Academy of Sciences, Beijing 100190, China

(Received 8 December 2020; revised 21 April 2021; accepted 26 May 2021; published 21 June 2021)

Ultrafast petawatt laser facilities require pulse compression strategies to deal with high-order dispersions. The third-order dispersion and especially the fourth-order dispersion need special compensation techniques. Quasiparametric amplification (QPA) has shown many benefits, such as high efficiency, and can bear the phase mismatch. In this paper we discuss the high-order dispersions induced in quasiparametric amplification and show the potential of the quasiparametric preamplifier with negligible pump depletion as a high-efficiency nonlinear phase compensator. We also discussed the high-order dispersions in QPA as a final stage amplifier where the pump is totally depleted and studied how those dispersions finally affect the amplified signal pulses.

DOI: 10.1103/PhysRevA.103.063513

I. INTRODUCTION

Petawatt light ($1\ \text{PW} = 10^{15}\ \text{W}$) sources have been applied for high-energy ion generation, laser-driven ion acceleration, and laser weak-field electron acceleration [1–4]. Optical parametric chirped-pulse amplification (OPCPA) is widely used in full-OPCPA PW-class laser facilities or as a front end in a hybrid PW-class laser for its potential in providing high-energy and ultrashort pulses [5–7]. A key task in high-intensity CPA or OPCPA laser is high-order dispersion management [8]. To achieve the Fourier-transform limit (F-T limit) in femtosecond petawatt facilities shorter than 30 fs, the third-order dispersion (TOD), as well as the fourth-order dispersion (FOD) must be well compensated [9]. The main source of TOD and FOD in petawatt laser facilities is from stretchers and compressors, i.e., grating pairs [10]. Several methods have been developed to compensate for the TOD and FOD induced by compressors and material dispersion, such as well-designed tiled gratings [11] or grism pairs [9]. These parts are designed to precompensate high-order dispersions as stretchers in PW-class laser facilities. Both TOD and FOD can be well compensated in an ideal system by configuring the tilt angle and position of gratings, as well as the angle of the incidence beam [12,13]. In a real system, an additional part is often necessary for compensating the residual nonlinear phase, such as an acousto-optic programmable dispersive filter (AOPDF) [14] or grism pairs [13], with intensity limitations and considerable intensity losses.

The nonlinear process in OPCPA has been discussed for over 20 years [15]. With the noncollinear optical parametric amplification (NOPA) technique, few-cycle pulses can be easily generated by the broadband parametric amplification [16]. However, the conversion efficiency of OPCPA is limited to 20% due to the back conversion [17]. To improve conversion efficiency, a new method is developed by an absorbing idler to suppress the back conversion called a quasiparametric chirped-pulse amplifier (QPCPA) [18–21]. Using this technique, the energy conversion efficiency can be performed up to 41%. Recent results show the potential of QPCPA in high efficiency and high stability amplification [19]. Meanwhile, to the best of our knowledge, no one considered the significant difference between the nonlinear phase induced by QPCPA and the nonlinear phase induced by OPCPA.

Here in this article, we will show a method for nonlinear spectral phase compensation via QPCPA. The high-order dispersions can be well compensated by adjusting the phase mismatch, by applying a QPCPA preamplifier module. In the following sections, we will discuss the theoretical models, giving a concise expression to the absorption-induced optical parametric phase under different conditions. At the same time, we will analyze the compensation process with the help of numerical simulation and discuss this method affecting pulse shaping in the parametric amplification process.

II. THEORATICAL ANALYSIS

The three-wave mixing process of OPCPA or QPCPA can be described by a set of coupled-wave equations which can be derived under the slowly varying envelope approximation from [22]:

$$\frac{\partial \boldsymbol{A}_s}{\partial z}+\sum_{n=2}^{\infty}\frac{(-j)^{n-1}}{n!}\left(\frac{\partial^n k_s}{\partial\omega^n}\right)\frac{\partial^n \boldsymbol{A}_s}{\partial\tau^n}+\mathcal{F}^{-1}\left(\frac{1}{2}\alpha_s(\omega)\right)*\boldsymbol{A}_s = j\frac{2d_{\text{eff}}\omega_s^2}{k_sc^2}\frac{\partial^2\boldsymbol{A}_i^*\boldsymbol{A}_p}{\partial\tau^2}\exp\left(-j\Delta k_0 z\right), \tag{1}$$

$$\frac{\partial \boldsymbol{A}_i}{\partial z}+\left(\frac{\partial k_i}{\partial\omega}-\frac{\partial k_s}{\partial\omega}\right)\frac{\partial \boldsymbol{A}_i}{\partial\tau}+\sum_{n=2}^{\infty}\frac{(-j)^{n-1}}{n!}\left(\frac{\partial^n k_i}{\partial\omega^n}\right)\frac{\partial^n \boldsymbol{A}_i}{\partial\tau^n}+\mathcal{F}^{-1}\left(\frac{1}{2}\alpha_i(\omega)\right)*\boldsymbol{A}_i = j\frac{2d_{\text{eff}}\omega_i^2}{k_ic^2}\frac{\partial^2\boldsymbol{A}_s^*\boldsymbol{A}_p}{\partial\tau^2}\exp\left(-j\Delta k_0 z\right), \tag{2}$$

*Corresponding author: ylchen@bjtu.edu.cn

$$\frac{\partial \boldsymbol{A}_p}{\partial z}+\left(\frac{\partial k_p}{\partial \omega}-\frac{\partial k_s}{\partial \omega}\right)\frac{\partial \boldsymbol{A}_p}{\partial \tau}+\sum_{n=2}^{\infty}\frac{(-j)^{n-1}}{n!}\left(\frac{\partial^n k_p}{\partial \omega^n}\right)\frac{\partial^n \boldsymbol{A}_p}{\partial \tau^n}$$
$$+\mathcal{F}^{-1}\left(\frac{1}{2}\alpha_p(\omega)\right)*\boldsymbol{A}_p=j\frac{2d_{\mathrm{eff}}\omega_p^2}{k_pc^2}\frac{\partial^2 \boldsymbol{A}_s\boldsymbol{A}_i}{\partial \tau^2}\exp\left(j\Delta k_0 z\right), \tag{3}$$

where $\boldsymbol{A}_m (m = s, i, p)$ are the complex pulse envelopes of the signal, the idler, and the pump light, respectively. τ is the normalized time with the pulse duration of signal t_s. $\Delta k_0 = k_s + k_i - k_p$ is the phase mismatch, $d_{\mathrm{eff}} = \chi_{\mathrm{eff}}{}^{(2)}/2$ is the effective nonlinear coefficient, c is the speed of light, and $\omega_{s,i,p}$ are the angular central frequency of the signal, the idler, and the pump, respectively. $\alpha_{s,i,p}(\omega)$ are the absorption coefficient. For OPCPA setup, $\alpha_{s,i,p}(\omega) = 0$, and in QPCPA, the absorption of idler $\alpha_i(\omega) \neq 0$. $F^{-1}(1/2\alpha_{s,i,p}(\omega))$ are the inverse Fourier transform in the temporal domain of the absorption coefficient of the signal, the idler, and the pump, respectively. $F^{-1}(1/2\alpha_{s,i,p}(\omega)) * A_{s,i,p}$ is the convolution of absorption and the complex pulse envelopes in the time domain.

Considering a noncollinear setup as shown in Fig. 1 with a small-signal approximation and ignoring the pump light depletion, the intensity-induced nonlinear spectral phase of the signal can be analytically expressed by Eq. (4), which is known as the optical parametric phase (OPP) [23]:

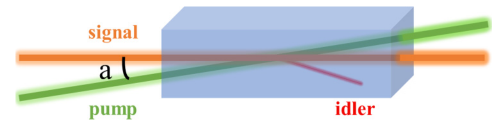

FIG. 1. Schematic of noncollinear QPCPA scheme. Here a is the angle between the signal beam and the pump beam.

$$\varphi_s^{\mathrm{OPP}}(\omega_s)\approx\begin{cases}-\arctan\left(\frac{\Delta k_0}{2\Gamma'}\right), & (\Delta k_0<2\,G)\\ -\arctan\left(\tan(hz)\frac{\Delta k_0}{2h}\right), & (\Delta k_0>2\,G)\end{cases}. \tag{4}$$

Here $\Gamma' = \sqrt{G^2 - \Delta k_0{}^2/4}$ and $h = \sqrt{-G^2 + \Delta k_0{}^2/4}$, where G is the gain factor. This approximation can hold when the depletion of pump intensity is less than 10% in our calculation.

Using the same presumption with Eq. (4) when $\Delta k_0 < 2G$ and including the absorption of the idler and the group delay of signal and idler, the absorption-induced OPP (AIOPP) can be expressed as

$$\begin{aligned}\varphi^{\mathrm{AIOPP}}&=-\tan^{-1}\left(\frac{C_1-\alpha_i g-4gf+\tan(gz)(C_2+2g\Delta k'-4g^2)-[C_1+\tan(gz)C_2]C_3}{C_2+2g\Delta k'-4g^2-\tan(gz)(C_1-\alpha_i g-4gf)+[C_2-\tan(gz)C_1]C_3}\right)\\&\approx-\arctan\left(\frac{\Delta k'-2g}{-\frac{\alpha_i}{2}+2f}\right)-gz\quad(\text{when } f\gg g\quad\text{and}\quad e^{-2fz}\ll 1),\end{aligned} \tag{5}$$

where the parameter $C_1 = \alpha_i g/2 + \Delta k' f$, $C_2 = 2f^2 + \alpha_i f/2 - g(\Delta k' - 2g)$, $C_3 = [(2f + \alpha_i/2)^2 + (2g - \Delta k')^2]G^{-2}e^{-2fz}$, the real part $f = \mathrm{Re}(\sqrt{G^2 - [\Delta k'/2 + (\alpha_i/4)j]^2})$, and g is the corresponding imaginary part. Here we define $\Delta k' - \Delta k_0 = k_s(\Delta\omega + \omega_s) + k_i(-\Delta\omega + \omega_i) - k_p(\omega_p) - \Delta k_0 = \sum_{n=1}^{\infty}(\frac{\partial^n \mathrm{k}_s}{\partial \omega^n} + (-1)^n\frac{\partial^n \mathrm{k}_i}{\partial \omega^n})(\Delta\omega)^n = \sum_{n=1}^{\infty}(\beta'_n)(\Delta\omega)^n$, $\Delta\omega = \omega - \omega_s$. Notice that the term $\sqrt{G^2 - [\Delta k'/2 + (\alpha_i/4)j]^2}$ is always complex when $\alpha \neq 0$. Without absorption, this term will be either a real number (when $\Delta k < 2G$) or an imaginary number (when $\Delta k > 2G$), and the AIOPP becomes OPP in this case. The influence of pump power to AIOPP is complex, which makes the AIOPP an extraordinarily complex expression. When the induced phase is much smaller than the gain factor in quantity, and $e^{-2fz} \ll 1$, the terms C_1 and C_3 will be much smaller than C_2 in Eq. (5), and the AIOPP can be approximated to $-gz$. In order to compare the difference between the spectral phase in OPCPA and QPCPA, the same term $-(\Delta k'\, z)/2$ is excluded. This term only contains dispersions up to the third order in the discussion and thus can be excluded when focusing on higher-order dispersions.

III. RESULTS AND DISCUSSION

First we discuss the case of QPCPA working with near-perfect phase matching when $\Delta k' \ll 2\sqrt{G^2 + \alpha_i{}^2/16}$ and $Gz \gg 1$. In this case, the real part $f \approx G'$ and the imaginary component g is simplified to the expression $-\alpha_i\Delta k'/8G'$. Here $G'(\omega) = \sqrt{G^2 - \Delta k'^2/4 + \alpha_i{}^2/16}$ and $G' = G'(\omega_s)$.

To qualitatively investigate the nonlinear spectral phase, we rewrite the AIOPP with Taylor expansion as

$$\varphi^{\mathrm{AIOPP}}=\varphi^{(0)\mathrm{AIOPP}}+\sum_{n=1}^{4}\frac{\varphi^{(n)\mathrm{AIOPP}}}{n!}(\Delta\omega)^n+o(\Delta\omega^5). \tag{6}$$

Consider an absorption spectrum with a Gaussian shape,

$$\alpha_i=\alpha_{i0}\exp(-(\omega-\omega_i)^2R^2). \tag{7}$$

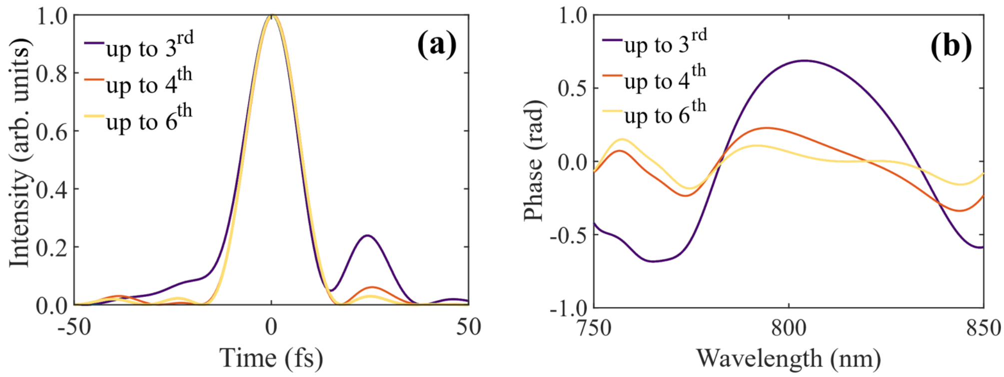

FIG. 2. (a) The amplified signal pulses with an initial pulse duration of 20 fs with dispersion control up to the third, fourth, and sixth order, respectively. (b) The corresponding spectral phase after dispersion control up to the third, fourth, and sixth order, respectively. The temperature increase is 100 K. The phase mismatch Δk_0 is zero at room temperature. The gain factor G is about 400 m^{-1}, and the crystal length is 20 mm.

When both α_{i0} and $\Delta k' \ll G$, we will get the expression of even-order and odd-order dispersions, assuming Gz » 1 by differentiating $\varphi^{\mathrm{AIOPP}} \approx -gz$ with respect to frequency ω:

$$\varphi^{(2n)\mathrm{AIOPP}} \approx (2n)!\left(\frac{\alpha_{i0}\beta'_{2n}}{4G}\left(-\frac{1}{\alpha_{i0}}+\frac{z}{2n!}\right)+(-1)^n\frac{\alpha_{i0}\Delta k_0 R^{2n}}{n!\,8G}z\right),\quad n \in \text{positive integers}, \tag{8}$$

$$\varphi^{(2n+1)\mathrm{AIOPP}} \approx (2n+1)!\left(\frac{\alpha_{i0}\beta'_{2n+1}}{4G}\left(-\frac{1}{\alpha_{i0}}+\frac{z}{(2n+1)!}\right)+(-1)^n\frac{\alpha_{i0}\beta'_1 R^{2n}}{n!\,8G}z\right),\quad n \in \text{positive integers}. \tag{9}$$

The even-order dispersions and odd-order dispersions are largely affected by the phase mismatch Δk_0 and the group velocity mismatch (GVM) β'_1 in QPCPA, respectively.

When a final stage amplifier uses QPCPA, where the pump is rapidly depleted and the idler absorption will cause a large temperature rise of about 100∼200 K, the temperature-induced phase mismatch can largely affect the high-order dispersions of the amplified signal. The shape of AIOPP is directly determined by the absorption spectrum. At the absorption maximum, there is the most phase accumulation. Away from the absorption center wavelength, the absorption decreases, so the phase accumulation decreases and eventually becomes the same with the standard OPCPA dispersion $-(\Delta k' z)/2$ (for example, a modified Gaussian-like phase spectrum). Such a spectral phase can be expressed as a sum of an infinite series that the higher-order dispersions have much greater contributions than lower orders in a broadband spectrum. Figures 2(a) and 2(b) show that when the temperature in the crystal increases by 100 K, the high-order dispersions containing FOD will increase the side peaks of the amplified signals unless a high-order dispersion control is applied. Not only the temperature increasing but also the pump depleting accelerates the accumulation of high-order dispersions.

On the other hand, in a preamplifier where the pump depletion can be ignored, the temperature-induced phase mismatch can be ignored, which means almost no AIOPP will be induced in a perfect phase-matching condition. Furthermore, because the phase mismatch Δk_0 can be easily controlled by adjusting the phase-matching angle, it provides a way to control high-order dispersions through phase mismatch or GVM. When the absorption spectrum centered in where the idler centered, the spectral phase could be easily analyzed. The nonlinear spectral phase in AIOPP is enlarged by the absorption and is much larger than in OPP in magnitude [Fig. 3(b)]. A large FOD or the fifth-order dispersion (FiOD) can be provided when α_{i0} and Δk are in the same quantity with G. This shows the possibility of controlling FOD and FiOD by compensating lower-order dispersions while keeping that the sum of higher-order dispersions has no contributions to the final spectral phase. The residual phase $o(\Delta\omega^5)$ can be estimated by $\phi^{(2)\mathrm{AIOPP}}$, $\phi^{(3)\mathrm{AIOPP}}$, and $\phi^{(4)\mathrm{AIOPP}}$ with the following approximations:

$$\varphi^{(2)\mathrm{AIOPP}} \approx -2!\frac{\left(G'^2-\alpha_{i0}{}^2/8\right)\alpha_{i0}R^2\Delta k_0}{8G'^3}z, \tag{10}$$

$$\varphi^{(3)\mathrm{AIOPP}} \approx -3!\frac{\alpha_{i0}R^2\beta'_1\left(G^2-\beta'_1{}^2/8\right)}{8G'^3}z, \tag{11}$$

$$\varphi^{(4)\mathrm{AIOPP}} \approx 4!\frac{\alpha_{i0}R^4\Delta k_0\left(G'^2-\alpha_{i0}{}^2/16\right)}{16\,G'^5}\left(G'^2-3\,\alpha_{i0}{}^2/16\right)z. \tag{12}$$

When the group velocity of signal and idler are matched, the residual spectral phase $o(\omega^5)$ can be kept to nearly zero in the spectrum range only when $\alpha_{i0} > G$. The following expression can be used to solve the proper residual-phase-eliminated conditions:

$$o(\omega^5) = \frac{\alpha_i\Delta k_0}{8\,G'(\omega)}z - \frac{\alpha_{i0}\Delta k_0}{8\,G'}z + \left(\frac{G'^2-(\alpha_{i0}/4)^2}{8\,G'^3}\right) \times\left[\omega^2 - \omega^4\left(\frac{G'^2-3(\alpha_{i0}/4)^2}{2\,G'^3}\right)R^2\right]\alpha_{i0}R^2\Delta k_0 z. \tag{13}$$

Residual spectral phase contributions should not have a large impact within the whole spectrum range to reach the F-T

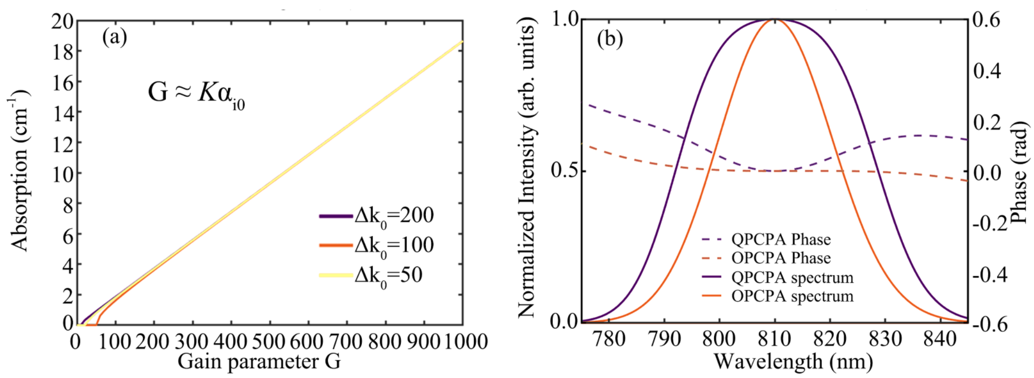

FIG. 3. (a) Absorption requirement for eliminating high-order dispersions within the range of $\pm 1.5\omega_0$. (b) Spectral phase of QPCPA with large phase mismatch. The curve is calculated with $z = 6$ mm, $G = 400\,\mathrm{m}^{-1}$, $\alpha_{i0} = 7.46\,\mathrm{cm}^{-1}$, and $\Delta k_0 = 200$ rad/m, with the absorption spectrum bandwidth equal to the bandwidth of the signal. The signal has a central wavelength of 810 nm, and the Fourier limit is 40 fs. The pump intensity is about $4\,\mathrm{GW/cm}^2$ with 532 nm.

limit. The exact number of FOD can only be calculated with the accurate expression in Eq. (5) when both α_{i0} and Δk_0 are comparable with G, even though Eq. (13) has enough accuracy to estimate the residual-phase-eliminated conditions.

Considering there is only group delay β_1' in the system to compensate the FiOD in the signal pulses, the high-order dispersion-eliminated conditions are almost the same with FOD compensation. The linear relation of G and α_{i0} is determined by the ratio K [Fig. 3(a)]. When the gain factor is nearly flat within the whole spectrum, the FOD control range is limited by the bandwidth of the absorption spectrum, showing the requirement of large-absorption-bandwidth nonlinear crystals. Recently, Yang *et al.* has reported the preparation process of $\mathrm{Pr:LiNbO_3}$ crystals with broadband absorption [24]. The ratio K depends on the spectrum range where the residual phase should be controlled, and a larger spectrum range requires a large absorption. On the other hand, the condition of eliminating $o(\omega^5)$ is less affected by Δk_0, β_1', and z, which ensures the feasibility of engineering the FOD and FiOD in a QPCPA preamplifier.

A NOPA geometry can offer a large gain bandwidth when the angle a between the signal beam and the pump beam has the following relationship: $a = \{\sin^{-1}[(1 - {\upsilon_s}^2/\upsilon i^2)/(1 + 2\upsilon_s k_s/\upsilon_i k_i + {k_s}^2/{k_i}^2)]\}^{1/2}$ [25], where υ_s and υ_i are the group velocity of signal and idler, respectively. FOD control by QPCPA requires the same phase mismatch within the spectrum so that NOPA is the best geometry compared to other geometries, such as quasi-phase matching or noncritical phase matching. By adjusting the crystal rotation to the desired angle in a NOPA geometry, it is able to adjust the FOD between -3×10^5 and $3 \times 10^5\,\mathrm{fs}^4$ and FiOD between -3×10^7 and $3 \times 10^7\,\mathrm{fs}^5$ in a 10-mm length nonlinear crystal (for example, Sm:YCOB) for ~40-fs signal pulses. When adjusting the FOD between -3×10^5 and $3 \times 10^5\,\mathrm{fs}^4$, the corresponding group delay dispersion (GDD) changes between -500 and $500\,\mathrm{fs}^2$. This GDD change can be easily compensated by adjusting grating pairs or prism pairs with only negligible effect on FOD, and the compensator can be designed as an adjustable device. Moreover, the beam direction will not change after the compensation of FOD. FiOD can be controlled with β_1' in the same way but will also cause gain narrowing when β_1' is too large.

To explore the properties of the QPCPA process in the temporal region, numerical simulations are done with Eqs. (1)–(3) based on the split-step Fourier-transform method combined with the Runge-Kutta method. This kind of modified split-step-Fourier method has been proved to be more accurate than the merely split-step-Fourier method [26].

Results show that the signal spectrum is broadened because the QPCPA gain factor is higher in the sides of the spectrum rather than higher in the center, and the gain factor is not largely affected by the phase mismatch. The QPCPA outputs shorter pulses than the original pulses after the compressor, as is shown in Fig. 4(a). Presuming a laser system with FODs of $3 \times 10^5\,\mathrm{fs}^4$ in 40-fs signal pulses, a QPCPA preamplifier can replace the OPCPA preamplifier to compensate FOD with $G = 320\,\mathrm{m}^{-1}$ and $\Delta k_0 \approx 300$ rad/m in 10-mm crystals. Figure 3(b) shows the residual phase can be well compensated in the whole spectrum range. To show the limit of the FOD control ability, a QPCPA with a gain factor $G = 640\,\mathrm{m}^{-1}$, $\Delta k_0 \approx 1000$ rad/m, and $\alpha_{i0} = 20\,\mathrm{cm}^{-1}$ is also calculated. In this parameter, a FOD up to $1.2 \times 10^6\,\mathrm{fs}^4$ can be well compensated. Although these FODs can be compensated by adjusting GDD in a certain degree as well, FODs can be better controlled with QPCPA phase modulation. The residual phase controlled by QPCPA is flatter than merely adjusting the GDD, which results in shorter pulses with a better pulse contrast (an order higher at ±400-fs scale). The AIOPP in a QPCPA preamplifier is not affected by the intensity of signal pulses when its intensity is in the small-signal region so that the AIOPP will not be affected by spatial beam profiles or intensity fluctuations of the signal.

Although the ideal phase compensation parameters we get from the above analytical expressions are a specific point, numerical results show the best phase compensation parameters can cover a wide range. We have calculated the pulse width of QPCPA output (t_{QPCPA}) and the corresponding Fourier-transform limits (t_{F-T}) among various conditions. $\Delta t = t_{\mathrm{QPCPA}} - t_{F-T}$ can be used to characterize the phase compensation in QPCPA. The ideal parameters in Fig. 4(a) are $G = 320\,\mathrm{m}^{-1}$ and $\Delta k_0 = 300$ rad/m, used to compensate for an initial FOD of $3 \times 10^5\,\mathrm{fs}^4$, and both the gain factor and phase mismatch can be adjusted in a wide range without

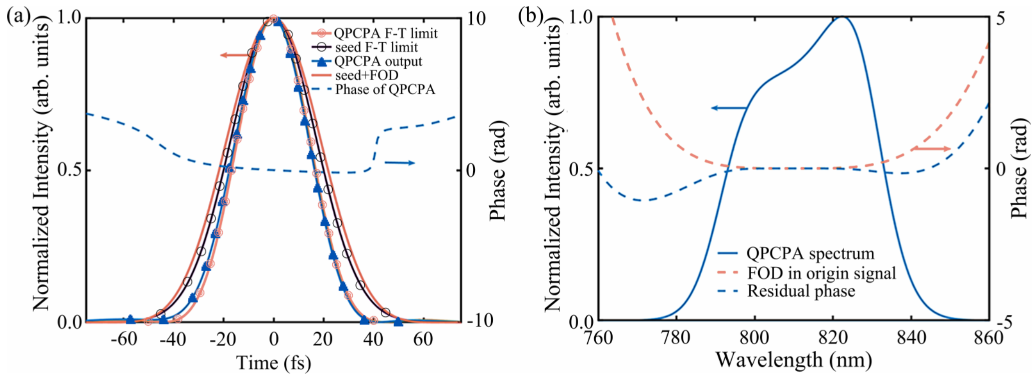

FIG. 4. The normalized signal pulse intensities and corresponding phase in the (a) temporal and (b) spectral region. The GDD of the QPCPA output is compensated, while the TOD is not compensated. The initial FOD is $3 \times 10^5\,\mathrm{fs}^4$, gain factor $G = 320.347\,\mathrm{m}^{-1}$, $\Delta k_0 = 298.81\,\mathrm{rad/m}$, and $\beta_1' = -1.098\,\mathrm{fs/mm}$. $\alpha_{i0} = 8\,\mathrm{cm}^{-1}$ and $z = 10\,\mathrm{mm}$.

large effects on the pulse duration. The widest adjustable range can be achieved in Fig. 4(a) when $\Delta k_0 \approx 300\,\mathrm{rad/m}$ and $G \approx 250\,\mathrm{m}^{-1}$. Although the FODs provided by QPCPA in these regions is far from the initial FOD, the residual phase after GDD compensation is still well controlled, which shows the high adaptability of this FOD compensation scheme. The thermal effect of idler absorption is less than 0.1 K in our calculation at a repetition rate of 100 Hz (calculated by the same method in Ref. [18] when the output signal is $\sim 70\,\mu\mathrm{J}$ and beam radius is 2.5 mm with an idler absorption of about $8\,\mathrm{cm}^{-1}$), and the phase mismatch caused by idler absorption can be ignored (Δk_0 changes $<1\,\mathrm{m}^{-1}$). Figure 5(b) shows the changes of Δt with the phase mismatch and the initial FOD in the signal pulses when the gain factor G is fixed at $320\,\mathrm{m}^{-1}$. The initial FOD between 0 and $3 \times 10^5\,\mathrm{fs}^4$ can be well compensated by varying the phase mismatch Δk_0.

A set of two-dimensional simulation results is shown in Fig. 6 to discuss the system stability towards pump power fluctuations or the pump intensity distributions. The pump beams in recent OPCPA have high-intensity uniformity with top-hat intensity profiles. QPCPA enlarges the high-order dispersions by idler absorption, and the AIOPP is sensitive towards the pump intensity, so QPCPA also requires a top-hat intensity profile pump laser. The QPCPA phase compensation process shows high stability towards the gain factors changes. To clarify this point, we show the comparison between the pulse duration with FOD compensated by QPCPA and the shortest pulse duration with FOD compensated by excessive GDD. Results show that the pulse duration can be kept to the F-T limit, even when the pump intensity decreases to 65% of the maximum. Spectrum modulation also plays an important role in the compression process. The intensity is concentrated in the two sides of the QPCPA spectrum, which is more insensitive towards even-order dispersions compared with a Gaussian-like spectrum. While pulse duration which is compressed by only excessive GDDs is sensitive towards spectrum changes, the pulses compressed by QPCPA are insensitive towards spectrum changes and can keep the pulses near the F-T limit when the pump intensity or signal intensity changes.

Although the compensating process is limited by absorption bandwidth, it is possible to compress a short pulse with narrower absorption bandwidth. We use both the difference between the pulse duration of QPCPA outputs and its F-T limits ($t_{\mathrm{QPCPA}} - t_{F-T}$) and the difference between the pulse duration of QPCPA outputs and the F-T limits of original signals $t_{\mathrm{QPCPA}} - t_{\mathrm{signal}}$ to characterize the pulse compression performances. Results show that a signal pulse of 20 fs can be well compressed by QPCPA with an 89-nm bandwidth absorption spectrum ($\Delta\omega_s/\Delta\omega_{ai} = 2$) and $1 \times 10^5\,\mathrm{fs}^4$ FOD [Fig. 7(a)]. If the 20-fs signal carries a large FOD (for example, $3 \times 10^5\,\mathrm{fs}^4$), the QPCPA cannot compress the pulse into

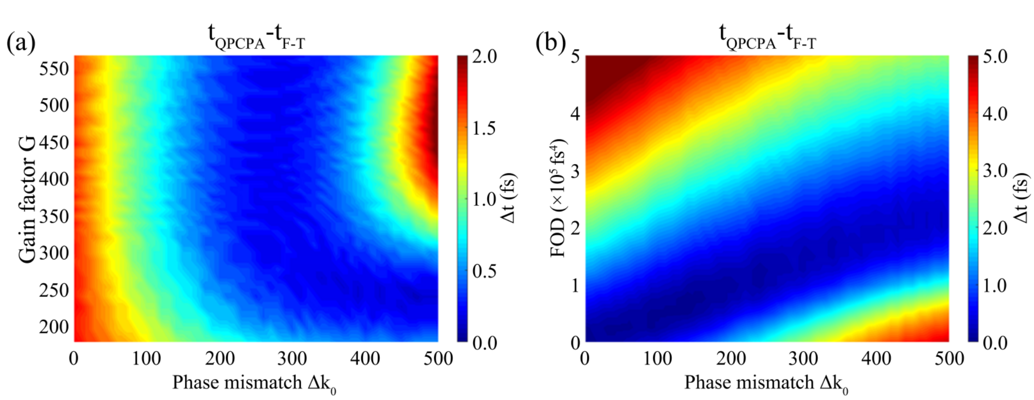

FIG. 5. $\Delta t = t_{\mathrm{QPCPA}} - t_{F-T}$ changes by varying the phase mismatch and (a) gain factor or (b) FOD, respectively. The Fourier-transform limit t_{F-T} is calculated with the corresponding QPCPA output spectrum. $\alpha_{i0} = 8\,\mathrm{cm}^{-1}$ and $z = 10\,\mathrm{mm}$.

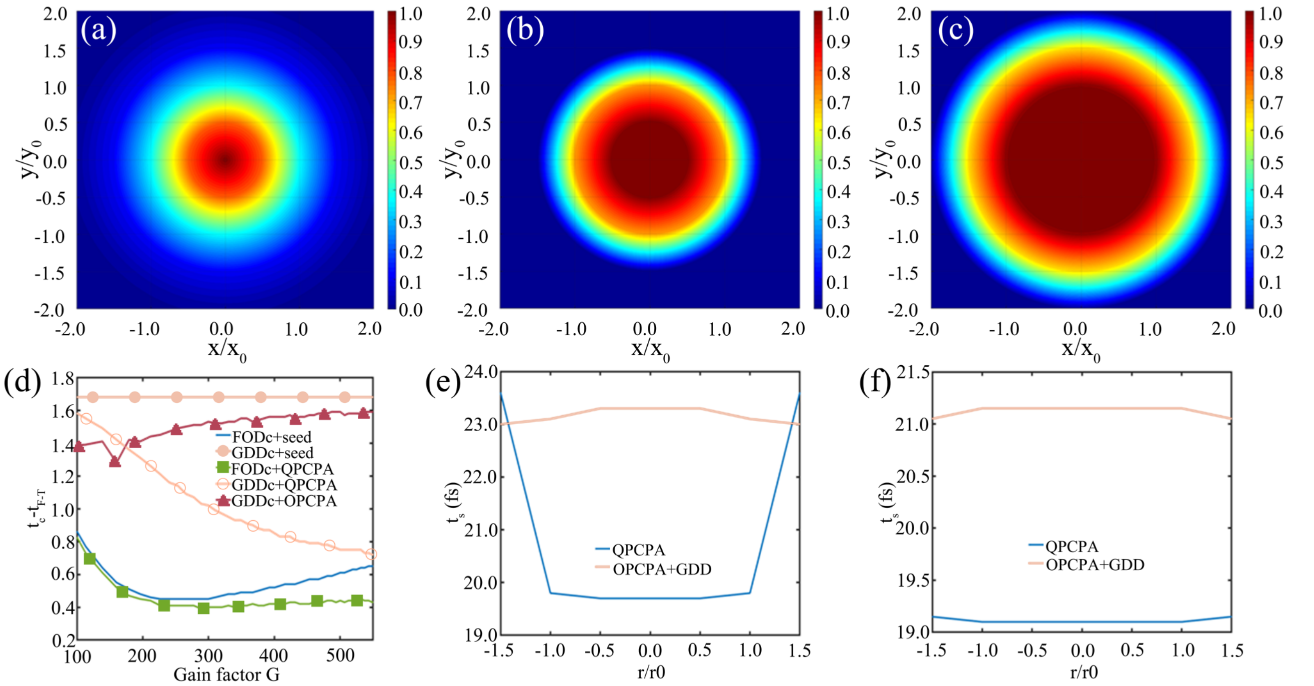

FIG. 6. (a)–(c) Intensity profile of the signal, a top-hat pump, and a top-hat pump with a larger beam radius, respectively. (d) Difference between the compressed pulse duration and the corresponding F-T limits. The compression GDD is fixed at $-652.66\,\mathrm{fs}^2$ in both QPCPA and excessive GDD phase compensation. The curves are for the QPCPA process (green) and the AIOPP added on the input Gaussian-like spectrum (blue); the FOD compressed by the GDD with a spectrum of QPCPA output (orange) and input (brown); the OPCPA process with excessive GDD compression (wine), respectively. (e)–(f) Compressed pulse duration calculated with a top-hat pump covering the center of the signal and the compressed pulse duration calculated with a top-hat pump covering nearly the whole signal, respectively. (e), (f) Calculated with $G = 450\,\mathrm{m}^{-1}$ and $\Delta k_0 = 180\,\mathrm{rad/m}$, and the pulse duration of the initial signal is 20 fs.

QPCPA F-T limits. But it is still able to reach the F-T limit of the original signal. To show the limitation of the FOD control of short pulses, a broadband absorption ($\Delta\omega_s/\Delta\omega_{ai} = 1$) with $\alpha_{i0} = 20\,\mathrm{cm}^{-1}$ is applied to compress $7.5 \times 10^4\,\mathrm{fs}^4$ of 20-fs pulses, which has an F-T limit of 15 fs after being QPCPA amplified [Fig. 7(b)]. The initial FOD with the QPCPA spectrum cannot be well compensated with merely excessive GDD without AIOPP because the spectrum is no longer a Gaussian shape and the residual phase is sensitive to this spectrum modulation. The initial FOD can be well compensated by adjusting the GDD with the help of AIOPP, and the pulse duration is able to reach the F-T limit. However, this FOD control method cannot support a pulse duration shorter than 15 fs in our calculation, because this method requires the same

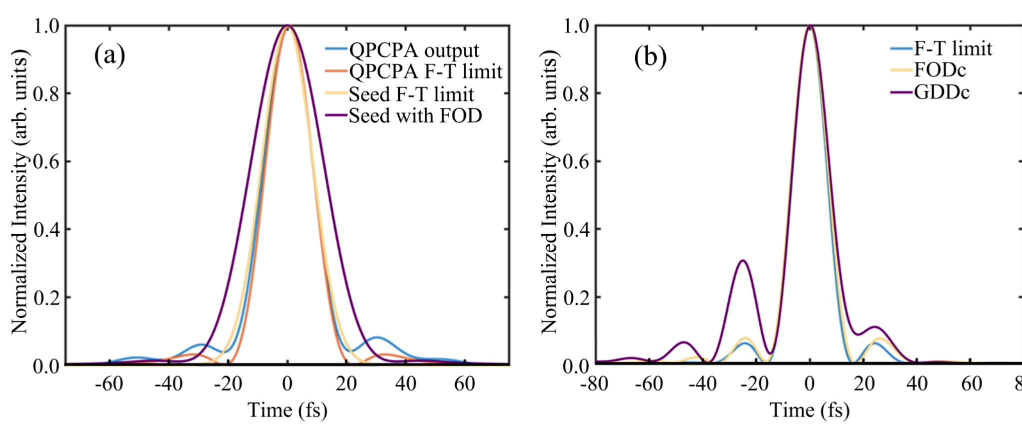

FIG. 7. (a) The normalized signal pulse intensities and corresponding phase intemporal region. The GDD and TOD of the QPCPA output are compensated. The initial FOD is $1 \times 10^5\,\mathrm{fs}^4$, gain factor $G = 320\,\mathrm{m}^{-1}$, and $\Delta k_0 = 200\,\mathrm{rad/m}$, $\alpha_{i0} = 7.67\,\mathrm{cm}^{-1}$, $z = 10\,\mathrm{mm}$. (b) Pulse duration calculated with an initial FOD $7.5 \times 10^4\,\mathrm{fs}^4$ with a 20-fs seed. $G = 640\,\mathrm{m}^{-1}$, $\Delta k_0 = 1000\,\mathrm{rad/m}$, $\alpha_{i0} = 20\,\mathrm{cm}^{-1}$, $z = 10\,\mathrm{mm}$. The F-T limit (blue) of QPCPA output is 15 fs. A well-compressed pulse (yellow) can be formed from QPCPA output, with GDD and TOD compensated. The pulse cannot be well compensated if considering the initial FOD compressed by merely GDD with such a spectrum without AIOPP.

phase mismatch within the whole spectrum, but a broader spectrum will lead to a rapid change of the phase mismatch, especially when Δk_0 should be kept large. Moreover, the absorption bandwidth would also be a problem. Even though an absorption spectrum formed by multipeaks may still be acceptable and the phase mismatch can be tuned by angular dispersions of signal, the design and adjusting will be complex and challenging. In the controllable region, this method has the potential to be a powerful tool in OPCPA design and adjusting

IV. CONCLUSION

In conclusion, we have shown that the quasiparametric amplification process will lead to strong high-order dispersions. In the small-signal region, the residual phase can be eliminated when the FOD is controlled, showing the great potential of the QPCPA preamplifier as an efficient high-order dispersion compensation module. The FOD can be tuned between -3×10^5 and $3 \times 10^5\,\mathrm{fs}^4$ for ~40-fs pulses and $\sim \pm 1 \times 10^5\,\mathrm{fs}^4$ for pulses shorter than 20 fs by adjusting the phase mismatch in a 10-mm-long nonlinear crystal. This phase compensation strategy shows a highly efficient, economic, and easy way of operation towards high-order dispersion management in ultrafast laser facilities. Numerical simulation results show that the signal spectrum is broadened because of the phase mismatch insensitive gain factor and thus could get a shorter pulse after the compressor. The compensator is very stable, which allows for wide-range changes in both phase mismatch and the pump intensity. Finally, we point out that the best bandwidth of the absorption spectrum is the same as the idler spectrum, and signal pulses longer than 15 fs with large FODs can be well compressed with the dispersion control.

ACKNOWLEDGMENTS

The work in this paper is partly of the research program of the Fundamental Research Funds for the Central Universities (No. 2019YJS209) and the National Nature Science Foundation of China (No. 51832009)

[1] S. K. Lee, H. T. Kim, I. W. Choi, and C. M. Kim, Exploration of strong field physics with multi-PW lasers, J. Korean Phys. Soc. **73**, 179 (2018).

[2] T. M. Jeong and J. M. Lee, Femtosecond petawatt laser, Ann. Phys. (Berlin) **526**, 157 (2014).

[3] T. Tajima and J. M. Dawson, Laser Electron Accelerator, Phys. Rev. Lett. **43**, 267 (1979).

[4] G. A. Mourou, T. Tajima, and S. V. Bulanov, Optics in the relativistic regime, Rev. Mod. Phys. **78**, 309 (2006).

[5] S. Gales, K. A. Tanaka, D. L. Balabanski, F. Negoita, and N. V. Zamfir, The extreme light infrastructure—Nuclear physics (ELI-NP) facility: New horizons in physics with 10 PW ultra-intense lasers and 20 meV brilliant gamma beams, Rep. Prog. Phys. **81**, 094301. (2018).

[6] F. Batysta, R. Antipenkov, T. Borger, A. Kissinger, J. T. Green, R. Kananavičius, G. Chériaux, D. Hidinger, J. Kolenda, E. Gaul, B. Rus, and T. Ditmire, Spectral pulse shaping of a 5 Hz, multi-joule, broadband optical parametric chirped pulse amplification frontend for a 10 PW laser system, Opt. Lett. **43**, 3866 (2018).

[7] X.-M. Zeng, K.-N. Zhou, Y.-L. Zuo, Q.-H. Zhu, J.-Q. Su, X. Wang, X.-D. Wang, X.-J. Huang, X.-J. Jiang, D.-B. Jiang, Y. Guo, N. Xie, S. Zhou, Z.-H. Wu, J. Mu, H. Peng, and F. Jing, Multi-petawatt laser facility fully based on optical parametric chirped-pulse amplification, Opt. Lett. **42**, 2014 (2017).

[8] Y. Zuo, K. Zhou, Z. Wu, X. Wang, N. Xie, J. Su, and X.-M. Zeng, Alignment of a petawatt-class pulse compressor with the third-order dispersion completely compensated, Laser Phys. Lett. **13**, 055302. (2016).

[9] Z.-Y. Li, C. Wang, S. Li, Y. Xu, L. Chen, Y.-P. Dai, and Y.-X. Leng, Fourth-order dispersion compensation for ultra-high power femtosecond lasers, Opt. Commun. **357**, 71 (2015).

[10] I. V. Yakovlev, Stretchers and compressors for ultra-high power laser systems, Quantum Electron. **44**, 393 (2014).

[11] V. V. Romanov and K. B. Yushkov, Configuration model of a grating pair pulse compressor, IEEE J. Selected Topics in Quantum Electronics **25**, 8800110 (2019).

[12] N. Forget, S. Grabielle, and P. Tournois, Tilted transmission grisms for pulse compression with dispersion control up to the fourth order, in *19th International Conference on Ultrafast Phenomena* (CLEO: Science and Innovations, United States, 2014), paper 09.Wed.P3.58.

[13] S. Li, C. Wang, Y.-Q. Liu, Y. Xu, Y.-Y. Li, X.-Y. Liu, Z.-B. Gan, L.-H. Yu, X.-Y. Liang, Y.-X. Leng, and R.-X. Li, High-order dispersion control of 10-petawatt Ti:Sapphire laser facility, Opt. Express **25**, 17488 (2017).

[14] M. Bock, L. von Grafenstein, U. Griebner, and T. Elsaesser, Generation of millijoule few-cycle pulses at 5 μm by indirect spectral shaping of the idler in an optical parametric chirped pulse amplifier, J. Opt. Soc. Am. B **35**, C18 (2018).

[15] A. Galvanauskas, A. Hariharan, D. Harter, M. A. Arbore, and M. M. Fejer, High-energy femtosecond pulse amplification in a quasi-phase-matched parametric amplifier, Opt. Lett. **23**, 210 (1998).

[16] S. Witte and K. S. E. Eikema, Ultrafast optical parametric chirped-pulse amplification, IEEE J. Selected Topics in Quantum Electronics **18**, 296 (2012).

[17] A. Vaupel, N. Bodnar, B. Webb, L. Shah, and M. Richardson, Concepts, performance review, and prospects of table-top, few-cycle optical parametric chirped-pulse amplification, Opt. Eng. **53**, 051507 (2014).

[18] J.-G. Ma, J. Wang, B.-J. Zhou, P. Yuan, G.-Q. Xie, K.-N. Xiong, Y.-Q. Zheng, H.-Y. Zhu, and L.-J. Qian, Broadband, efficient, and robust quasi-parametric chirped-pulse amplification, Opt. Express **25**, 25149 (2017).

[19] J.-G. Ma, J. Wang, P. Yuan, G.-Q. Xie, K.-N. Xiong, Y.-F. Tu, X.-N. Tu, E.-W. Shi, Y.-Q. Zheng, and L.-J. Qian, Quasi-parametric amplification of chirped pulses based on a Sm^{3+}-doped yttrium calcium oxyborate crystal, Optica **2**, 1006 (2015).

[20] D.-X. Hu, Y.-D. Tao, J.-G. Ma, J. Wang, P. Yuan, H.-Y. Zhu, and L.-J. Qian, Comparative study on coherent noise in optical

parametric and quasi-parametric chirped-pulse amplification, Opt. Commun. **464**, 125461 (2020).

[21] X.-N. Tu, K.-N. Xiong, S. Wang, Y.-Q. Zheng, and E.-W. Shi, Large size Sm-doped YCOB crystal grown by Bridgman method for QPCPA application, J. Cryst. Growth **535**, 125543 (2020).

[22] B. J. Zhou, J. G. Ma, J. Wang, D. L. Tang, G. Q. Xie, P. Yuan, H. Y. Zhu, and L. J. Qian, Nonlinear spectral phase induced by optical parametric chirped-pulse amplification, Phys. Rev. A **95**, 033841 (2017).

[23] H. J. Bakker, P. C. M. Planken, L. Kuipers, and A. Lagendijk, Phase modulation in second-order nonlinear-optical process, Phys. Rev. A **42**, 4085 (1990).

[24] C. L. Yang, X. N. Tu, S. Wang, K. N. Xiong, Y. L. Chen, Y. Q. Zheng, and E. W. Shi, Growth and properties of Pr^{3+} doped $LiNbO_3$ crystal with Mg^{2+} incorporation: A potential material for quasi-parametric chirped pulse amplification, Opt. Mater. **105**, 109893 (2020).

[25] J. Zheng and H. Zacharias, Non-collinear optical parametric chirped-pulse amplifier for few-cycle pulses, Appl. Phys. B **97**, 765 (2009).

[26] A. Willinger and G. Eisenstein, Split step Fourier transform: A comparison between single and multiple envelope formalisms, J. Lightwave Technology **30**, 2988 (2012).